

Quantifying Uncertainty of Digital Elevation Models Derived from Topographic Maps

Qihao Weng

Department of Geography, Geology, and Anthropology, Indiana State University,
Terre Haute, IN 47809, USA

Abstract

This paper explores a methodology for quantifying the uncertainty of DEMs created by digitising topographic maps. The origins of uncertainty in DEM production were identified and examined. The uncertainty of DEM data was quantified by computing a vector total of Root Mean Square Error (RMSE) from the source map, sampling and measurement errors, and the interpolation process. Distributional measures including accuracy surfaces, spatial autocorrelation indices, and variograms were also employed to quantify the magnitude and spatial pattern of the uncertainty. The test for this methodology utilises a portion of a 1:24 000 topographic map centred on Stone Mountain in northeastern Georgia, USA. Five DEMs, constructed with different interpolation algorithms, are found to have the total RMSE ranging from 4.39 to 9.82 meters, and a highly concentrated pattern of uncertainty in rugged terrain. This study suggests that the RMSE provides only a general indicator of DEM uncertainty. Detailed studies should use distributional measures to understand how the uncertainty varies over a surface.

Keywords: DEM, uncertainty, origins; distributional measures

1 Introduction

Two methods are frequently employed for obtaining digital elevation model (DEM) data: cartographic digitising and photogrammetric (analytical or digital) methods. The cartographic digitising method is widely used since topographic maps are usually available. The basic procedure involves the transformation of contour lines on existing maps into digital coordinate data using manual or automatic digitizers. A surface is then fitted to these point observations in interpolation of the elevation at every grid point. Alternatively, an automatic raster scanner is used with the vectorization technique. This method is straightforward, and the coverage can be very large. However, the general quality of the derived DEM is poor unless great efforts are made to extract terrain characteristic features and break lines as well (Ackermann, 1994).

The quality of a DEM is dependent upon a number of interrelated factors, including the methods of data acquisition, the nature of the input data, and the methods employed in generating the DEMs (Shearer, 1990). Of all these factors, data acquisition is the most critical one. Previous studies on DEM data acquisition have focused either on examination of generation method(s), or on case studies of accuracy testing (Ackermann, 1978; Ebner and Reiss, 1984; Torlegard *et al.* 1987). These studies are not adequate, however, for the purpose of understanding uncertainty (an indicator used to approximate the discrepancy between geographic data and the geographic reality that these data intend to represent) associated with DEM data and the propagation of this uncertainty through GIS based analyses. The development of strategies for identifying, quantifying, tracking, reducing, visualising, and reporting uncertainty in DEM data are called for by the GIS community (Zhu, 1997; Fisher, 1999; Heuvelink, 1999; Veregin, 1999).

The objectives of this study are: (1) to understand the sources and reasons for uncertainty in DEMs produced by cartographic digitising; and (2) to develop methods for quantifying the uncertainty of DEMs using distributional measures.

2 Measurement of DEM Uncertainty

Measurement of errors in DEMs is often impossible because the true value for every geographic feature or phenomenon represented in a geographic data set is rarely determinable (Goodchild *et al.* 1994; Hunter *et al.* 1995). Uncertainty, instead of error, should be used to describe the quality of a DEM. Quantifying uncertainty in DEMs requires comparison of the original elevations (e.g., elevations read from topographic maps) with the elevations in a DEM surface. Such a comparison results in height differences (or residuals) at the tested points. To analyse the pattern of deviation between two sets of elevation data, conventional ways are to yield statistical expressions of the accuracy, such as the root mean square error, standard deviation, and mean. In fact, all statistical measures that are effective for describing a frequency distribution, including central tendency and dispersion measures, may be used, as long as various assumptions for specific methods are satisfied.

The most widely used measure is the Root Mean Square Error (RMSE). It measures the dispersion of the frequency distribution of deviations between the original elevation data and the DEM data, mathematically expressed as:

$$RMSE_z = \sqrt{\frac{1}{n} \sum_{i=1}^n (z_{di} - z_{ri})^2} \quad (1)$$

Where: Z_{di} is the i^{th} elevation value measured on the DEM surface;
 Z_{ri} is the corresponding original elevation;
 n is the number of elevation points checked.

The larger the value of the RMSE, the greater the discrepancy between the two data sets. When the true values such as ground truth are used as the reference data, the “uncertainty” becomes “error”. Accuracy is the reverse measurement of error. The accuracy of a DEM can be defined as the average vertical error of all potential points interpolated within the DEM grid (Ackermann, 1996). In other words, it is the vertical root-mean-square accuracy of all points (infinitely many) interpolated in the DEM grid.

The main attraction of the RMSE lies in its easy computation and straightforward concept. However, this index is essentially a single global measure of deviations, thus incapable of accounting for spatial variation of errors over the interpolated surface (Wood, 1996). This index fails, besides, to reveal any information about the mean deviation between the two measures of elevation, neither the form of frequency distribution such as balance between small and large deviations and skewness of the distribution (Wood, 1996). Most interpretations of the RMSE value assume a zero mean deviation, which is often invalid (Li, 1993a; Li, 1993b; Monckton, 1994). Moreover, the magnitude of the RMSE value depends on the variance of a true elevation distribution, and is subject to the influence of relative relief and scale of measurements (Wood, 1996). To correctly report and compare the RMSE values for areas with different relative relief values a composite index such as RMSE-to-contour density ratio should be developed and utilised in order to minimise the influence of this “natural” variance (Gao, 1997).

3 Uncertainty from Elevation Measurements for Topographic Maps

The vertical accuracy of topographic maps with which terrain elevations are photogrammetrically measured depends on the base-height ratio, the relationship of the ground distance between successive exposures of photographs to the flying height. The larger the ratio, the higher the heighten accuracy. For a particular flying height, camera focal length and angular coverage are the two factors determining the base-height ratio. Therefore, theoretically speaking, super-wide-angle photography is better than wide- and narrow-angle photography for height measurements. In practice, however, wide-angle photography is most frequently used, since a compromise must be made between heighten accuracy and the requirements for good scale and resolution (Petrie, 1990).

If a particular base-height ratio is set, the accuracy of height measurements is then largely limited by flying height. Petrie (1990) reports that the expected accuracy of spot heights using wide-angle photography will be between 1/5,000 and 1/15,000 of the flying height, depending on the type of stereo-plotter used. For example, from flying heights in the range of 1 to 15 km, the heighten accuracy will range from 0.1 to 3.0 meters (RMSE).

There are four data sampling patterns generally employed in obtaining elevation measurements: systematic, random, composite sampling, and contouring. Systematic sampling is a grid-based measurement of spot heights in a regular geometric pattern, square, rectangular, or triangular. In contrast, random sampling measures heights at significant points selected by the photogrammetrist, e.g., on hilltops, along break lines and streams. Composite sampling combines elements of both of the above approaches. The final method is contouring, which systematically measures contours over the whole area of the stereo model supplemented occasionally by the measurement of spot heights along terrain break lines. This mode of measurement consistently yields significantly lower accuracy than the first three methods (Petrie, 1990; Shearer, 1990). The minimum possible contour interval will lie between 1/1,000 and 1/2,000 of the flying height. The expected or specified accuracy of such measurements is that 90 percent of all the points shall be within half of the contour interval. This photogrammetric criterion has been applied to the United States National Map Accuracy Standards. Thus, if the error in the vertical dimension is assumed to be a normal distribution, then the vertical RMSE can be computed as follows:

$$1.645\text{RMSE} = \text{contour interval} / 2 \quad (2)$$

Solving for the RMSE, then:

$$\text{RMSE} = 0.304 * \text{contour interval} \quad (3)$$

Table 1 summarises the relationship between flying height, minimum possible contour interval and the heighten accuracy within one standard deviation (assume that the mean is the true value). If we assume that the camera used to take the source aerial photos has a focal length of 15 cm (wide-angle, most commonly used), then the relationships between photo scale, contour interval, and vertical accuracy can be established.

Table 1. Flying height, minimum possible contour interval, and heighting accuracy

Flying height (m.)	Minimum possible contour interval (m.)	RMSE (90%)
1 000	0.5~1.0	0.25~0.5
5 000	2.5~5.0	1.25~2.5
10 000	5.0~10.0	2.50~5.0
15 000	7.5~15.0	3.75~7.5

Source: Petrie, 1990. Compiled by the Author.

4 Uncertainty from Spatial Interpolation

4.1 Methods for Assessing the Uncertainty

It has been demonstrated that DEM accuracy can vary to a certain degree with different interpolation algorithms and interpolation parameters (Eklundh and Martensson, 1995; Weng, 1998). Five commonly used spatial interpolation

algorithms are examined and compared in this study. They include inverse distance squared (Davis, 1986), minimum curvature (Briggs, 1974), modified Shepard's method (Shepard, 1968; Wang, 1990), radial basis function (Hardy, 1990), and triangulation with linear interpolation (Wang, 1990). These interpolators convert randomly spaced data points into regularly gridded data points, which can then be used to generate DEM surfaces. These interpolators can be classified as either an exact or approximate algorithm, if the original data points are preserved on the interpolated surface (Wren, 1975; Lam, 1983).

The test site is selected from a 7.5-minute (1:24,000) USGS topographic map that has a contour interval of 20 feet. It is located in Stone Mountain, Georgia, a hill of moderate relief composed of granite bedrock, and covers a rectangular area of 13,000 by 16,000 feet (Fig. 1). The maximum and minimum elevation of this site is 1683 and 800 feet respectively, resulting in a relative relief of 883 feet. The mean elevation is 976.79 feet, with the standard deviation of 205.93 feet. These statistical indicators should be compared when a new study area is selected, because the accuracy of interpolation is, to a certain degree, subject to the influence of terrain complexity (Ackermann, 1996; Gao, 1997).

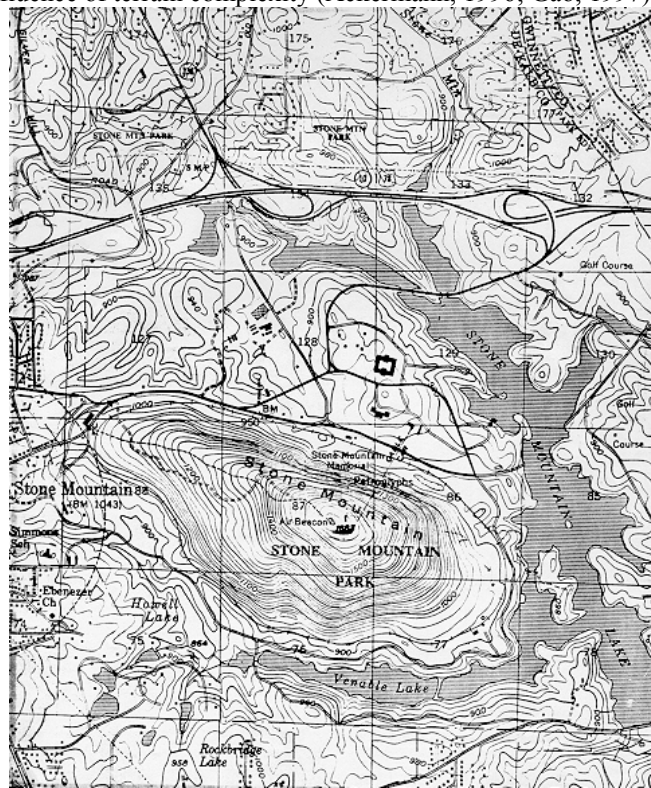


Fig. 1. Test site: Stone Mountain of the northeastern Georgia

The data capture process involves using the CAPTURE (R-WEL, Inc.) and

entering point elevations into the database by keyboard. The rule for the selection of points is to distribute them evenly throughout the area examined. Ideally, the points should be those with exact locations identified, such as benchmarks, spot heights, or road intersections. Alternatively, the points where a geographic feature intersects with a contour line are used. The initial data set includes a total of 50 points. With an increment of 50 randomly distributed points overtime, each subsequent data set is generated. At the end, eight data sets with the density of 50, 100, 150, 200, 250, 300, 350, and 400 points become ready for gridding.

The interpolation package used in this study is SURFER. The following three questions are taken into account in evaluating the accuracy of interpolation of elevation data: (1) Among the interpolation algorithms examined, which will produce the most accurate result, statistically and spatially? (2) How does grid resolution influence the accuracy of interpolation? (3) Does data point density have an impact on interpolation uncertainty? If so, what is the relationship between data point density and interpolation uncertainty? To answer these questions, the RMSE of the residuals is computed to reveal the closeness of an interpolated surface to the reality. Check points were picked up along the contour lines of the topographic map and compared with the corresponding elevations on an interpolated surface.

4.2 Test Results

In assessing the accuracy of various interpolation algorithms, the same grid resolution, i.e., 50 meters, is used. Table 2 shows the result of the interpolation. Among the interpolators, the radial basis function (RMSE=6.6628) generates nearly identical result. Triangulation with linear interpolation algorithm provides the worst interpolation, producing the largest total deviation (RMSE=9.5403). The contour map created has distinct triangular faces, indicating that too few data points have been used for the interpolation. The inverse distance squared algorithm generates a reasonably high statistical accuracy (RMSE=6.8404), comparable to kriging and radial basis function. If the RMSE is the only concern, then the modified Shepard's method is the best interpolator (RMSE=3.9448). However, both the modified Shepard's method and the inverse distance algorithm tend to produce a "bull's eye" pattern. Minimum curvature produces acceptable smooth interpolated surfaces, but its statistical accuracy is low (RMSE=8.6937). The selection of parameters for interpolation is listed in Table 3. It should be noted that the changes in interpolation parameters might improve or worsen the statistical performance of an interpolator (Weng, 2001).

Table 2. Effect of different input densities on the quality of interpolation

Input data points	RMSE (meters)				
	Inverse distance squared	Minimum curvature	Modified Shepard's method	Radial basis function	Triangulation
50	7.4302	8.5602	3.6579	7.8448	7.7563
100	6.8536	8.4038	3.5165	7.2330	7.6556
150	6.7879	8.3581	3.2428	6.7818	7.4228
200	6.7663	8.2080	2.7764	6.7567	7.2442
250	6.6793	8.1543	2.1534	6.0605	7.1802
300	6.3638	8.0112	2.1210	5.7965	7.0263
350	5.8988	7.9794	2.7277	6.1366	8.4747
400	6.8404	8.6937	3.9448	6.6632	9.5403

Table 3. Interpolation parameters used

Algorithms	Interpolation parameters
Kriging with linear variogram	C = 292; A = 5.7 Nugget effect: Error variance = 0; Micro variance = 0
Inverse distance squared	Drift type: No Drift $\beta = 3$; $\delta = 0$
Minimum curvature	Max residual = 0.08; Max iteration = 10,000
Shepard's method	Smoothing = 0
Radial basis functions	$R^2 = 0.01$
Triangulation with linear interpolation	N.A.

5 Spatial Distribution of DEM Uncertainty

5.1 Measurement of Spatial Uncertainty of DEMs

It is necessary to note that DEM uncertainty reported by the RMSE assumes a uniform error value for an entire DEM surface. This assumption is often not true. Many authors have suggested that the distribution of errors in DEMs will show some forms of spatial pattern (Guth, 1992; Li, 1993a; Wood and Fisher, 1993;

Monckton, 1994). The best way to observe and analyze the spatial pattern of uncertainty is to have a graphical representation - creating an accuracy surface. This representation has the advantage of clearly indicating where serious, and perhaps anomalous errors occur. Comparison of such a surface, for example, with a plot of the original input contours, can be extremely informative with respect to the occurrence and magnitude of errors in relation to such factors as the terrain slopes and distribution of input data (Shearer, 1990).

Furthermore, a spatial autocorrelation index can be computed to measure the extent of error clustering. When interval/ratio data are of concern, then either the Moran's I or the Geary's C can be used to measure spatial autocorrelation. The former is more commonly used in mapping accuracy. Both are inversely related, and often imply the same results (Griffith and Amrhein, 1991). Moran's I statistic is computed as follows:

$$I = \frac{n \sum_{u=1}^n \sum_{v=1}^n w_{uv} (dz_u - \overline{dz})(dz_v - \overline{dz})}{\sum_{u=1}^n (dz_u - \overline{dz})^2 \sum_{u=1}^n \sum_{v=1}^n w_{uv}} \quad (4)$$

Where: dz_u is the deviation between the two models for each cell;
 dz_v is the deviation between the two models for some neighbouring cells;
 w_{uv} is the weighting given to neighboring cells; and
 \overline{dz} is the average deviation between the two models.

The value of this statistic usually ranges from -1 to 1, with the value 1 indicating similar value clustering, 0 random pattern, and -1 dissimilar value clustering.

An accuracy surface was created to show the spatial pattern of uncertainty resulted from the interpolation (Fig. 2), in which the magnitude of uncertainty is represented by means of contours. It is clear from these maps that uncertainty tends to cluster in rugged areas of the test site where elevation changes rapidly, especially around the crest of the mountain. All surfaces have a value of the Moran's index larger than 0.8, indicating a reasonably high degree of clustering. However, a close look at these diagrams reveals that some interpolators do a better job than others in terms of revealing the systematic errors that result from under-representation of rugged areas. The modified Shepard's method produces the least degree of clustering. The minimum curvature algorithm, on the other hand, generates a great deal of clusters around the Stone Mountain. In between them are kriging, radial basis function, inverse distance, and triangulation with linear interpolation. A correlation between the RMSE and the Moran's index gives a coefficient of 0.87, indicating that statistically better-interpolated surfaces may result in less error clustering.

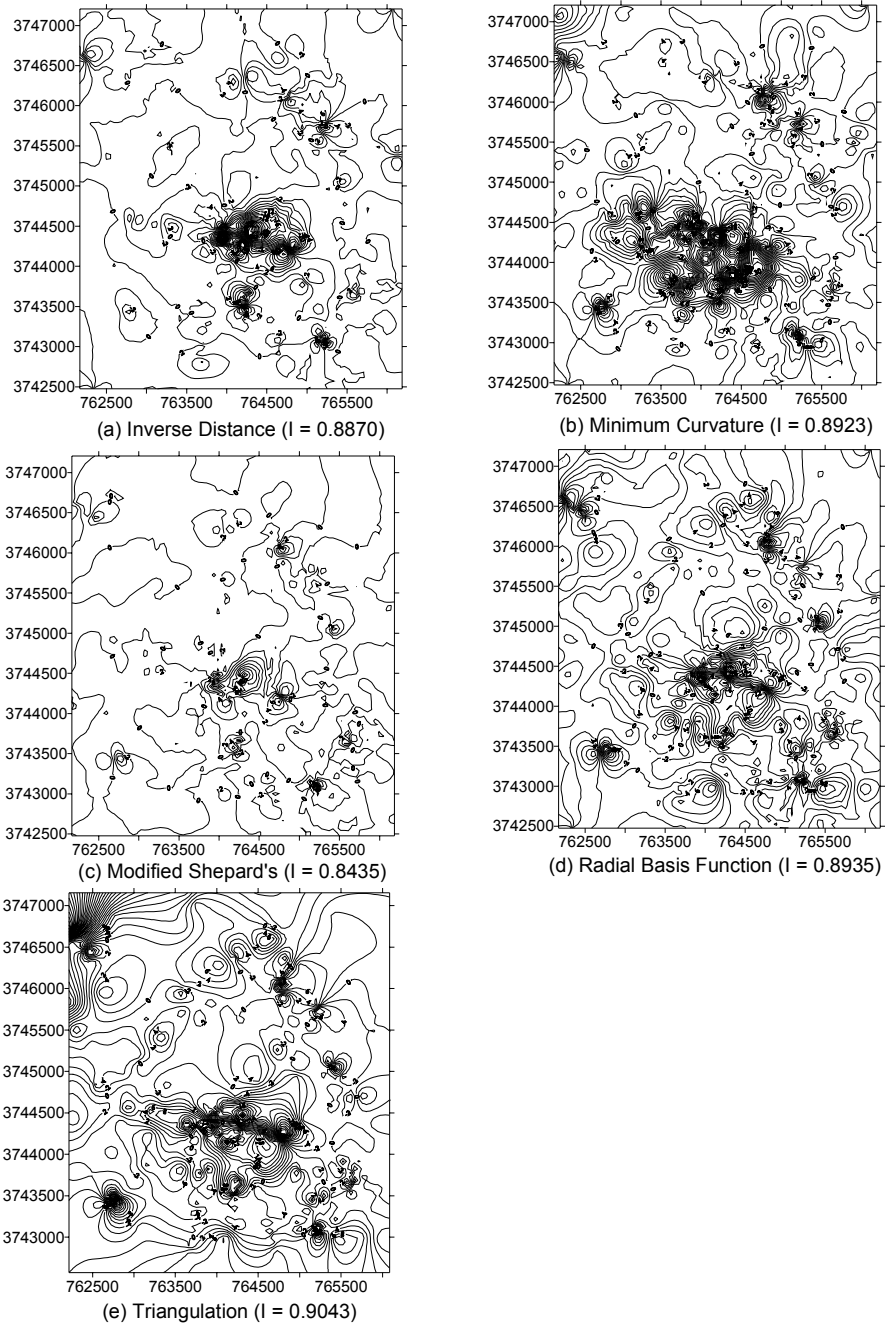


Fig. 2. Accuracy surfaces of the DEMs of Stone Mountain

5.2 Variogram Modelling Spatial Variability of the Residuals

The apparent pattern of clustering in the elevation residuals suggests that there exists an underlying spatial trend in the residual values in each accuracy surface. A common tool to investigate this spatial trend is the empirical variogram (Houlding, 1994). Variogram modelling allows for describing and measuring how difference in residual value changes with distance and direction. The classical variogram function is essentially a measure of dissimilarity between two observations at a separation distance (the lag) h apart, and can be defined as (Carr, 1995):

$$\gamma(h) = \frac{1}{2n(h)} \sum_{i=1}^n (z_i - z_{i+h})^2 \quad (5)$$

where z_i and z_{i+h} are the values of residual at locations i and $i+h$, and n is the number of pairs considered. Applying this equation to the residual data, six empirical variograms are constructed (of which five are shown in Fig. 3). These variograms show the spatial variance of the residual values at every 200 feet. In order to evaluate the spatial variance at any separation distance, a continuous function (curve) must be fitted to these point observations. Table 4 shows the results of model fitting and parameters estimated.

The exponential model gives us the best quality of fit for the accuracy surfaces of kriging, modified Shepard's method, and radial basis function; while the spherical model gives the best fit for the accuracy surfaces of inverse distance squared, minimum curvature, and triangulation with linear interpolation. The estimated range for the models, over which the influence of spatial dependency of the residual values is in effect, differ from 320 to 1300 feet. This is equivalent to 0.16 to 0.65 inch in the map. The highest range goes to triangulation with linear interpolation (range = 1300 ft), because this algorithm basically does not account for the underlying trend in the data. The remaining five interpolation algorithms have an average range of 508 feet (i.e., a quarter inch in the map). Beyond these ranges, the increase in separation distance will no longer cause a corresponding systematic increase in the average squared difference between pairs of residual values. This parameter relates closely to the terrain complexity that a variogram model attempts to represent. The information listed in Table 4 therefore provides also a guide for determining input data sampling interval and density.

The estimated nugget takes into account both sampling and measurement error and microscale variation (the spatial variation occurring at distance closer than the sample spacing). This study finds that microscale variation in all of the models equals to zero. Since the minimum separation distance in all the six models is small (Fig. 3), it is safe to conclude that sampling and measurement error are primarily related to the nugget effect, which has a range of 3.43 to 23 feet. Based on the value of nugget effect, the standard deviation of the sampling and measurement error (RMSE) can be calculated. It is estimated to be from 1.85 to 4.79 feet, or from 0.56 to 1.46 meters.

Table 4. Estimated variogram models for the interpolation residuals

Interpolators	Estimated variogram model	Anisotropy (ratio; angle)
Kriging with linear variogram	$\gamma(h) = \begin{cases} 11 & h=0 \\ 11+29*[1-\exp(-\frac{h}{570})] & h>0 \end{cases}$	2; 81.88
Inverse distance squared	$\gamma(h) = \begin{cases} 7 & h=0 \\ 7+11*[\frac{1.5h}{450}-0.5*(\frac{h}{450})^3] & 0 < h < 450 \\ 18 & h \geq 450 \end{cases}$	1; 0
Minimum curvature	$\gamma(h) = \begin{cases} 23 & h=0 \\ 23+68*[\frac{1.5h}{700}-0.5*(\frac{h}{700})^3] & 0 < h < 700 \\ 91 & h \geq 700 \end{cases}$	2; 169.1
Modified Shepard's method	$\gamma(h) = \begin{cases} 3.43 & h=0 \\ 3.43+2.5*[1-\exp(-\frac{h}{320})] & h>0 \end{cases}$	2; 51.38
Radial basis functions	$\gamma(h) = \begin{cases} 13 & h=0 \\ 13+24*[1-\exp(-\frac{h}{500})] & h>0 \end{cases}$	2; 76.59
Triangulation with linear interpolation	$\gamma(h) = \begin{cases} 22 & h=0 \\ 22+37*[\frac{1.5h}{1300}-0.5*(\frac{h}{1300})^3] & 0 < h < 1300 \\ 59 & h \geq 1300 \end{cases}$	2; 117.6

6 Discussion

The uncertainty of digital elevation models resulting from cartographic digitising is related to three aspects: the elevation measurements for the topographic map, sampling and measurement error, and the interpolation process. Assuming the uncertainty from each source is an independent vector, the total DEM uncertainty can be computed as follows:

$$RMSE_{total} = \sqrt{[(RMSE_m)^2 + (RMSE_s)^2 + (RMSE_i)^2]} \quad (6)$$

where $RMSE_m$, $RMSE_s$, and $RMSE_i$ are the uncertainty from the source map, from the sampling and measurement error, and from the interpolation process respectively. With the Eq. 6, the overall quality of the DEMs for the Stone Mountain with different spatial interpolation algorithms can be assessed. More

generally, an error budget table can be created to give an estimate of the uncertainty from various sources (Table 5). This table provides the reader with some guidelines for creating DEMs with the cartographic digitising method. However, this table and the findings of this paper should be applied with caution before the following points have been fully considered:

- (1) Correlation of uncertainty. The uncertainty in the source map and the uncertainty caused by the interpolation are often correlated. High uncertainty tends to concentrate in rugged terrain areas in both sources. The Eq. 6 needs to be adjusted to account for this correlation in any future research effort.
- (2) Point density and distribution. The accuracy of spatial interpolation of elevations is subject to input data point density and distribution, among many other factors. The analysis should be extended into the impact of different data collection patterns (e.g., random vs. systematic; significant points vs. contouring). Equally important is the problem of how to take the complexity of terrain into account to determine point density and distribution. Comparative studies may be conducted by using different input data density for different degrees of roughness in a surface or by taking break lines.
- (3) Scale. Scale issue comes into terrain analysis in many ways. The scale of a source map has a direct impact on the quality of DEM generated. The accuracy of terrain parameters and features derived from DEMs exhibits scale dependencies (Hutchinson and Gallant, 1999). Moreover, the degree of clustering of DEM uncertainty may vary at different scales (Monckton, 1994). There are also problems of how the terrain characteristics of a multi-scale can be mathematically described. The analysis should be extended into more complicated types of terrain in different geomorphologic settings at different scales.
- (4) Variation in interpolation parameters. The variation in interpolation parameters may significantly improve or worsen the DEM accuracy. Some exemplary questions of further investigation include: How does the RMSE of residual values change as the smoothing parameter of the radial basis function becomes larger, and how will it change with a larger smoothing parameter in the modified Shepard's method, and how will it decrease as the weighting power of inverse distance algorithm becomes larger? Are these effects related to terrain complexity and scale?

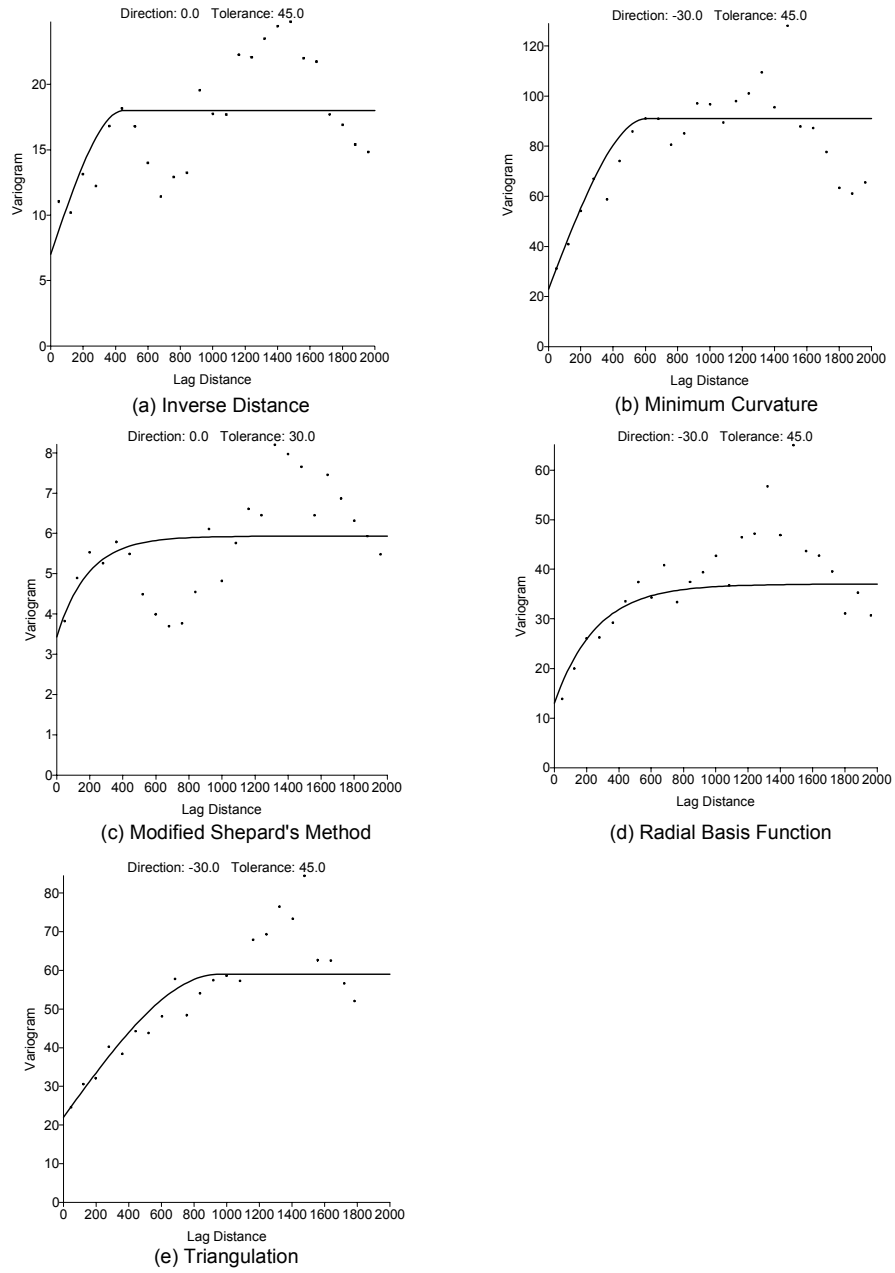


Fig. 3. Exponential/spherical fit to variograms on interpolation residuals

7 Conclusions

Table 5. Error budget for the DEMs based on 1:24 000 topographic maps

Error sources	Range of RMSE (meters)
Source map	1.85
Interpolation	
-Variation in interpolation algorithm	3.9448 ~ 9.5403
-Variation in input data density (50 ~ 400 points)	5.7960 ~ 7.8322
-Variation in grid resolution (10 ~100 meters)	2.2675 ~ 9.8154
Sampling and measurement	0.5645 ~ 1.4618
Total	4.3935 ~ 9.8226

This paper has addressed issues related to the uncertainty of DEMs based on the cartographic digitising method. It is suggested that the uncertainty of a DEM may be quantified by calculating a vector total of the RMSE from the source map, from the sampling and measurement error, and from the interpolation.

The RMSE of the source map may be computed as $RMSE = 0.304 * \text{contour interval}$, assuming a 90 percent rule for 1/2 contour interval errors. Both the positional and heighten accuracy of a topographic map are specified based on photogrammetric and surveying criteria, and they, in turn, define the contour interval of the map.

The determination of the uncertainty from the interpolation requires computing the value of residuals between the interpolated and the original elevations at tested points. The magnitude of uncertainty from the spatial interpolation is subject to many factors, but primarily to interpolation algorithm parameters and input data point density and distribution at a given grid resolution.

The RMSE alone is not sufficient for quantifying DEM uncertainty, because this measure rarely addresses the issue of distributional accuracy. To fully understand and quantify the DEM uncertainty, spatial accuracy measures, such as accuracy surfaces, indices for spatial autocorrelation, and variograms, should be used. The uncertainty is found concentrated in rugged terrain areas, although the five interpolators produce various spatial patterns of clustering. The degree of clustering is substantially high in all surfaces, as indicated by the Moran's index. Variogram modelling allows for quantitatively assessing the spatial variability of the residual data, and for calculating the RMSE that resulted from the sampling and measurement errors.

References

- Ackermann F (1978) Experimental investigation into the accuracy of contouring through DTM. In: Proceedings of Digital Terrain Modelling Symposium. St. Louis, pp 165-192
- Ackermann F (1994) Digital elevation models: techniques and applications, quality standards, development. In: ISPRS (ed) Proceedings of the Symposium on Mapping and Geographic Information Systems. University of Georgia, Athens, Georgia, pp 421-432
- Ackermann F (1996) Techniques and strategies for DEM generation. In: Greve C (ed) Digital Photogrammetry: An Addendum to the Manual of Photogrammetry. American Society of Photogrammetry and Remote Sensing, Falls Church, VA, pp 135-141
- Briggs IC (1974) Machine contouring using minimum curvature. *Geophysics* 39(1): 39-48
- Carr JR (1995) Numerical Analysis for the Geological Sciences. Prentice Hall, Englewood Cliffs, NJ
- Davis JC (1986) Statistics and Data Analysis in Geology (Second Edition). John Wiley and Sons, New York
- Ebner H, Reiss P (1984) Experience with height interpolation by finite elements. *Photogrammetric Engineering and Remote Sensing* 50(2): 177-182
- Eklundh L, Martensson U (1995) Rapid generation of digital elevation models from topographic maps. *International Journal of Geographic Information Systems* 9(3): 329-340
- Fisher P (1999) Models of uncertainty in spatial data. In: Longley PA, Goodchild MF, Maguire DJ, Rhind DW (eds) *Geographical Information Systems (Volume 1): Principles and Technical Issues (Second Edition)*. John Wiley and Sons, New York, pp 191-205
- Gao J (1997) Resolution and accuracy of terrain representation by grid DEMs at a micro-scale. *International Journal of Geographic Information Science* 11(2): 199-212
- Goodchild MF, Buttenfield BP, Wood J (1994) Introduction to visualizing data quality. In: Hearshaw HM, Unwin DJ (eds) *Visualization in Geographic Information Systems*. John Wiley and Sons, New York, pp 141-149
- Griffith DA, Armhein CG (1991) *Statistical Methods for Geographers*. Prentice-Hall, Englewood Cliffs, NJ
- Guth P (1992) Spatial analysis of DEM error. In: Proceedings of ASPRS/ACSM Annual Meeting. American Society of Photogrammetry and Remote Sensing, Washington DC, pp, 187-196
- Hardy RL (1990) Theory and applications of the multiquadratic-biharmonic method. *Computers and Mathematics with Applications* 19: 163-208
- Heuvelink G (1999) Propagation of error in spatial modeling with GIS. In: Longley PA, Goodchild MF, Maguire DJ, Rhind DW (eds) *Geographical Information Systems (Volume 1): Principles and Technical Issues (Second Edition)*. John Wiley and Sons, New York, pp 207-217
- Houlding SW (1994) *3D Geoscience Modeling: Computer Techniques for Geological Characterization*. Springer-Verlag, New York
- Hunter GJ, Caetano M, Goodchild, MF (1995) A methodology for reporting uncertainty in spatial database products. *Journal of the Urban and Regional Information Systems Association* 7: 11-21

- Hutchinson MF, Gallant JC (1999) Representation of terrain. In: Longley PA, Goodchild MF, Maguire DJ, Rhind DW (eds) *Geographical Information Systems (Volume 1): Principles and Technical Issues (Second Edition)*. John Wiley and Sons, New York, pp 105-124
- Lam SN (1983) Spatial interpolation methods: a review. *The American Cartographer* 10 (2): 129-49
- Li Z (1993a) Theoretical models of the accuracy of digital terrain models: An evaluation and some observations. *Photogrammetric Record* 14(82): 651-659
- Li Z (1993b) Mathematical models of the accuracy of digital terrain model surfaces linearly constructed from square gridded data. *Photogrammetric Record* 14(82): 661-673
- Li Z (1994) A comparative study of the accuracy of digital terrain models (DTMs) based on various data models. *ISPRS Journal of Photogrammetry and Remote Sensing* 49(1): 2-11
- Monckton C (1994) An investigation into the spatial structure of error in digital elevation data. In: *Innovations in GIS 1*. Taylor and Francis, London, pp 201-211
- Petrie G (1990) Photogrammetric methods of data acquisition for terrain modelling. In: Petrie G, Kennie TJM (eds) *Terrain Modeling in Surveying and Engineering*. Whittles Publishing Services, Caithness, pp 26-48
- Shearer, JW (1990) The accuracy of digital terrain models. In: Petrie G, Kennie TJM (eds) *Terrain Modeling in Surveying and Engineering*. Whittles Publishing Services, Caithness, pp 315-336
- Shepard D (1968) A two dimensional interpolation function for irregularly spaced data. In: *Proceeding 23rd National Conference ACM*. Brandon/Systems Press, Princeton, pp 517-523
- Torlegard K, Ostman A, Lindgren R (1987) A comparative test of photogrammetrically sampled digital elevation models. In: *Transactions of the Royal Institute of Technology, Photogrammetric Reports Nr 53*, Sweden
- Veregin H (1999) Data quality parameters. In: Longley PA, Goodchild MF, Maguire DJ, Rhind DW (eds) *Geographical Information Systems (Volume 1): Principles and Technical Issues (Second Edition)*. John Wiley and Sons, New York, pp 177-189
- Wang L (1990) *Comparative Studies of Spatial Interpolation Accuracy*. Master thesis, Department of Geography, University of Georgia
- Weng Q (1998) Comparative assessment of spatial interpolation accuracy of elevation data. In: *Proceedings of 1998 ACSM Annual Convention and Exhibition*. Baltimore, Maryland
- Weng Q (2001) A methodology for conceptualizing and quantifying uncertainty of Digital Elevation Models. In: Forer, P, Yeh A, He J (eds) *Advances in GIS Research III: Towards Holistic Spatial Data Handling*. Springer-Verlag, Berlin
- Wood J (1996) *The Geomorphological Characterisation of Digital Elevation Models*. Ph.D. thesis, Department of Geography, University of Leicester, Leicester, UK
- Wood J, Fisher P (1993) Assessing interpolation accuracy in elevation models. *IEEE Computer Graphics and Applications* 13(2): 48-56
- Wren AE (1975) Contouring and the contour map: a new perspective. *Geographical Prospecting* 23: 1-17